Nat. Volatiles & Essent. Oils, 2021; 8(6): 3868-3879

Tailored Manufacture Of Chitosan-Silver Nanoparticles (Agnp) Composite Membranes: Preparation, Characterization, And Antibacterial Agent

Ni Nyoman Rupiasih[1] , Wayan Gede Suharta[2] , and Made Sumadiyasa[3]

[1,2,3]Department of Physics, Faculty of Mathematics and Natural Sciences, Udayana University, Bali, Indonesia 80361

Abstract

Chitosan powder and silver nanoparticles (AgNP) are materials of great interest to researchers due to their excellent properties and wide application potentials. Many studies have been done to improve the utilization of chitosan powder in various fields. One is improving the characteristics of chitosan (Ch) membranes. In this work, the fabrication of chitosan composites membranes was attained by using Ag nanoparticles as fillers for a potential method in improving the physical properties. The composites membranes were made by a casting technique using a solvent of acetic acid. The mass of AgNP used was 10, 100, and 1000 µg. Those membranes called as Ch-AgNP10, Ch-AgNP100, and Ch-AgNP1000, respectively. A pure chitosan membrane was also made, named Ch. The physical property of those membranes have been measured by numerous methods including Barrett-Joyner-Halenda (BJH), X-ray diffraction (XRD), dynamic mechanical analysis (DMA), and water uptake capacity. Functional group analysis was performed using a Fourier Transform Infra-Red (FTIR) Spectrophotometer. The membranes have also been tested for the antibacterial properties against E. coli, a gram-negative and S. aureus, gram-positive bacteria using Kirby-Bauer inhibition zone method. The results indicated that the diameter of the pores of those composites membranes is smaller than Ch membrane, however, the diameter of the pores increased with increasing the quantity of Ag nanoparticles added. The longest elongation is showed by Ch-AgNP10. The highest value of elastic modulus (E), the tensile strength (TS), and the capacity of the water uptake is indicated by Ch-AgNP100. The XRD pattern showed two characteristic peaks 2θ=14.89o and 21.27o which correspond to the chitosan and some new peaks at 2θ around 29o, 39o, and 47o, that corresponding to Ag nanoparticles. The functional groups detected in the composite membranes included OH and NH stretch, CH stretch, C=O, C-O-C, and metal oxide (Ag-O) which mostly moved to the longer wavelength compared with Ch membrane. The composite membranes have antibacterial effect to the E. coli, but not to S. aureus. Therefore referring to these results, this study provided basic knowledge for the manufacturing chitosan-AgNP composites membranes with tailored characteristics with its application.

Keywords: Chitosan powder, silver nanoparticles (AgNP), composites membrane, physical property, antibacterial activity

Introduction

The rising requirement to build eco-friendly polymer materials with better mechanical properties and strength, has directed to the improvement of combine materials (composite) which natural polymer as a main component. Chitosan (Ch) is a natural polymer attained by the elimination of the acetyl group of chitin [1], where chitin itself is produced by living organisms which mostly find in exoskeletons of crustacean such as shrimp and crab shell, also in cell walls of fungi [2]. Chitosan is shows excellent properties, such as biocompatibility and biodegradability, nontoxic, antibacterial, physiological inert and bioactivity [3]. The antibacterial, biocompatible, and nontoxic characteristics of chitosan make it applicable in various human health fields [4], [5].

Chitosan is recognized as a multipurpose natural material which exist in various forms for example micro-crystalline powders, membrane, fiber, solutions, and lotions [6]–[9]. It is an outstanding material to make membranes as a result of its mold ability, reactivity, and hydrophilicity. Also chitosan is biocompatible and has good mechanical properties [10]. It comprises a big number amine (NH_2) and hydroxyl radicals (OH) groups. These radical groups can be adapted by various ligands and also simply be linked with other molecules. The amine groups can be made a chain-linked chitosan membrane which useful for restriction of biomolecules [11]. Various applications of membranes that made of chitosan have been studied including anti-adhesion membranes for post-operative applications, preparing controlled-release medicine membranes, chitosan membrane for immobilization, artificial skin [12], for the elimination of Cu^{2+} from water-based solution [13], adsorption and desorption of different metal ions [14], in vitro evaluation of bioactivity [15], restriction of an oxidoreductase (glucose oxidase) and considered their prospective practice in biosensors [16]. Alternatively, the prospective use options for chitosan membranes in the technological areas are very wide and therefore there is an ongoing search for membrane materials that have some particular properties or have varied uses that can be simply adapted for chosen goods.

The blend of polymer with nanoparticles, that named as nano-composites create a new type of materials which are predictable to show well characteristics [17]. Basically, the combination of inorganic particles addicted to the chitosan matrix is addressed to enhance mechanical characteristics and, sometime to give bioactivity to a chemically inert material [18]. The particles can be used as fillers for chitosan composites such as bioactive ceramic nanoparticles (nano-biomaterials), bioactive glass, and metal nanoparticles. The usage of nano-fillers is notable as a result of their high surface area, giving great a shared boundary across that generate high forming common boundary strength. This will enhance the mechanical characteristic of the composite; improve the weight transfer ability, and reducing the fatal catastrophe produced by bad weight transfer [19], [20].

Silver nanoparticles are the greatest general antimicrobial materials because of their strong biocide result to microorganisms that has been applied for a long time ago to avoid and medicate numerous diseases [21]. It has been known as a disinfectant and antimicrobial agent that is quite safe [22]. In the form of nanoparticles, silver exhibit outstanding antimicrobial effect, even at a low concentration. This is due to the large surface-to-volume ratio [23]. They are shown low immunological response and cytotoxicity, also low cost [24].

Both chitosan and Ag are antibacterial substances so chitosan-AgNP composite shows a stronger antibacterial effect than chitosan or Ag itself. It reported that chitosan-AgNP composite is more actual counter to bacteria than the chitosan itself [25], [26]. Chitosan is an excellent material to produce membranes which applicable in various fields especially related to human health [4]. So, in this work, we tried to couple both remarkable properties of the materials, chitosan powder and Ag nanoparticles to get new types of membranes with better performances. Here we report the manufacture and the characteristics of chitosan-AgNP composites membranes for a possible technique in refining mechanical characteristics and antibacterial effect.

Materials and Methods

Materials

The chitosan (Ch) powder used is extracted from prawn with characteristics of the average molecular weight of 900,000, DD (degree of deacetylation) of 87.4%, and the solvability in acetic acid 1% is 99.4%. Sodium hydroxide (NaOH) and acetic acid were analytical grade (p.a.) and were applied straightly without any refinement. Distilled water (DW) was applied in solutions preparation. The silver nanoparticles used are a biosynthesized product by using Sambiloto leaf extract which characteristics are the SPR (surface Plasmon resonance) wavelength of 423 nm and pores size of about 10-30 nm. It crystalize is FCC (face center cubic) and the lattice parameter 'a' of 4.03 Å [27].

Membranes Preparation

The chitosan membrane and composites membranes were prepared by a solution casting technique. The chitosan powder was used as the matrix, 1% acetic acid (v/v) as a solvent, and Ag nanoparticles powder as filler. The amounts of Ag nanoparticles used were 10, 100, and 1000 µg. The solution casting technique was following the protocol in our previous works [1], [28]. Briefly, the chitosan membrane was made by mixing 2% wt chitosan powder with acetic acid, stirring gently at 37 °C up to a dope solution (a homogeneous solution) obtained. The dope solution was cast on a glass plate of 18.5 x 24.0 cm^2, and then dried at ambient temperature. The dried membrane was dipped into 1 MNaOH, soaked for 12 minutes, washed by distilled water three times, and dried over at ambient temperature. Lastly, it is got a dry chitosan membrane, named Ch membrane. The composite membranes are made by the same procedure, by adding AgNP with different amounts. The composite membranes made, named Ch-AgNP10, Ch-AgNP100, and Ch-AgNP1000, respectively.

Characterization Methods

The crystal structures of the membranes were recorded using a PAN alytical XRD with the wavelength of the radiation source of 0.154 nm, current 35 mA, and 40 kV. The scanning was conducted on dry membranes in the range of 7º to 60º with a resolution of 0.02º.

The pore size and pore density of those membranes made were examined by the BJH (Barrett-Joyner-Halenda) technique using Nova 1200e as described in [1]. The tensile test of the membranes was examined using DMA (dynamic mechanical analysis) using ASTM D5630 or ISO 3451. The measurements conducted on dry membranes at ambient temperature.

The water uptake ability was measured as the protocol described in [1] and [28]. Mainly, the dry membranes were cut in circular form with a diameter of about 3.5 cm and weighed (m_d). Further, it soaked in 20 ml of distilled water for some time, pick up, then removed the excess water from the surface of the membranes with filters paper, and finally weighed (m_w). The water uptake ability of the membranes calculated by (1) [1], [28].

$$Water\,uptake\,(\%) = \frac{m_w - m_d}{m_d} x100\% \qquad (1)$$

The infrared (IR) spectra of Ch and composite membranes were recorded to analyze the functional group present in all membranes. The spectra have scan in the region of 400 to 4000 cm^{-1} using a FTIR (Fourier Transform Infrared) spectrophotometer, IR Prestige-21. The spectra have scan with a resolution of 4 cm^{-1} and averaged ten scans.

The antibacterial activity was conducted using the Kirby-Bauer inhibition zone method to Gram-positive S. aureus and Gram-negative E. coli as reported in [29] and [30]. The procedure is. The medium used was nutrient agar (NA) and it prepared on petri dishes with a diameter of 9 cm. The S. aureus and E. coli were inoculated after appropriate dilution. Square membranes with a size of about 1.0 cm^2 were placed on the inoculated culture medium. The cultures were incubated for 24 h at 37 °C and then the diameter of the clear zones formed around the membrane is sized. All experiments were replicated three times and it is reported on the average values.

Results and Discussion

X-ray Diffraction Analyses

The XRD measurement is used to determine the crystal form of the Ch membrane and Ch-AgNP composite membranes made. The XRD patterns show in Fig. 1. In order to observe the crystal form changes that occurred on the Ch membrane and the Ch-AgNP composite membranes, XRD analysis was also carried out on chitosan powder and AgNP powder, the results are shown together in Fig. 1. Broad XRD peaks of chitosan powder, chitosan membrane, and composite membranes below 30° indicate the semi-crystalline form of the main constituent of chitosan. Chitosan powder showed two characteristic peaks around 2θ=11.81° and 20.75° appropriate to the hydrated and anhydrous crystals, respectively. Those peaks correspond to the crystallographic planes (002) and (101) [4], [25], [31]. The XRD graph of AgNP powder shows peaks at 2θ=38,18°, 45,81°, and 64,87° corresponding to the crystallographic planes (111), (200), and (220) [27]. The XRD graph of Ch membrane was almost the same as that of chitosan powder, with two characteristic peaks 2θ=14.89° and 22.51°, where both moved toward higher diffraction. This showed that the crystal forms of chitosan were not changed [31].

Fig.1. X-ray diffraction graphs of chitosan and AgNP powders, chitosan and chitosan composite membranes (Ch-AgNP10, Ch-AgNP100 and Ch-AgNP1000) in dry condition.

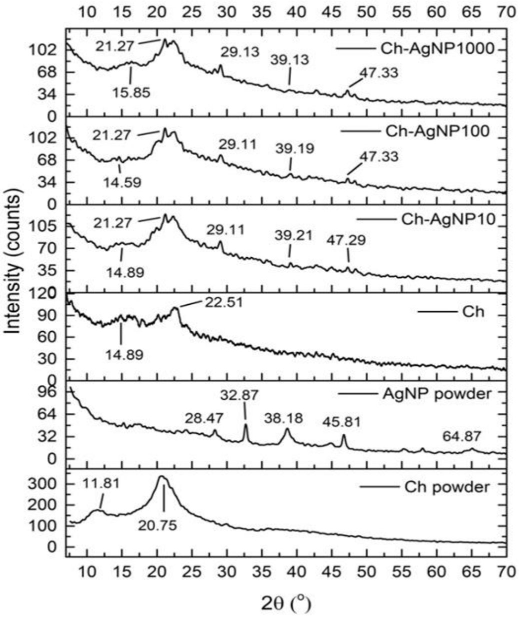

The XRD graphs of Ch-AgNP composite membranes also showed two characteristic peaks 2θ=14.89° and 21.27°, and some new peaks at 2θ around 29°, 39°, and 47°. The new peaks observed on composite membranes corresponded to AgNP that was added as filler on the composite membranes [4], [16]. The new peaks moved toward lower diffraction angle compared with the AgNP powder. This indicated the interaction between the chitosan and the AgNP occurred so it formed cross-linked composite membranes [31]. This finding is supported by the results of FTIR analysis, where there is a peak around 580-600 cm^{-1} which is a metal oxide (Ag-O) group [4], [26].

The Ch membrane, the prominent peak at 22.51° corresponds to intense hydrogen bonds inside or between molecules of chitosan [8]. Meanwhile, on the composite membranes, the peak observed at 21.27°

it's moved toward a smaller angle where the intensity increased. The characteristic peaks $2\theta=14.89^{o}$ are almost constant, but the intensity decreased. Those changes show a partial rupture of the hydrogen bonds. This showed a considerable reduction in the stiffness of chitosan backbones, which gives to pointedly improve the water-uptake ability of composite membranes, especially Ch-AgNP10. This finding is supported by the tensile test and swelling test of the Ch-AgNP10 and Ch-AgNP100, which is described below.

The Pore Density and Pore Size of Composites Membranes

The pore density and pore size of Ch membrane and chitosan composites membranes (Ch-AgNP10, Ch-AgNP100, and Ch-AgNP1000) obtained using the BJH method are shown in Fig. 2a and 2b. Fig. 2a shows the pore diameter of chitosan composites membranes are smaller compared with Ch membrane, but it is increased as more amount of AgNP is added (10 to 1000 µg). Fig. 2b shows that, the pores density of composites membranes increased from $3.40\text{x}10^{16}$ to $12.9\text{x}10^{16}$ pores/m^3 for Ch-AgNP10 and Ch-AgNP100, then decreased to $3.36\text{x}10^{11}$ pores/m^3 for Ch-AgNP1000. The decreased in the density of the pore may be due to the increase in the number of AgNP added. Based on the IUPAC convention for porosity nomenclature (1972), all membranes are included in the mesoporous group with pore diameters ranging from 30.60 to 38.51 Å, which can be used in the microfiltration process [33].

Tensile Test

The tensile test measurements were used to determine tensile strength (TS), the elongation-at-break (ε), and elastic modulus (E) of the membranes. Figure 3a shows stress-strain curves of Ch and composite membranes (Ch-AgNP10, Ch-AgNP100, and Ch-AgNP1000). From the stress-strain curves, Fig.3a, it obtained elastic modulus (Fig. 3b), tensile strength (Fig.3c), and elongation-at-break of each membrane as shown in Fig. 3d. Tensile strength is the maximum stress that can be held by the membranes before breaking. Elongation-at-break is the size of elasticity of the membranes that can be measured as specific defects of the membranes before damage [1]. Fig. 3b indicates that Ch-AgNP100 has the highest elastic modulus and tensile strength but its elongation at break is very small (Fig. 3d). This shows that the Ch-AgNP100 is the most rigid membrane compared to other composite membranes and Ch membranes. The longest elongation at break (in Fig. 3d) is indicated by Ch-AgNP10, also it has good values in elastic modulus (Fig. 3b) and tensile strength (Fig. 3c). This indicates that Ch-AgNP10 is a strong and ductile membrane. It can be concluded that the Ch-AgNP100 is the strongest membrane, while the strong and ductile membrane is the Ch-AgNP10. So AgNP have an impact on the tensile strength of the Ch-AgNP composite membranes made. Adding the number of AgNP to 100 µg will increase the strength of the membrane composites formed but decrease the ductility, thus decreasing the ability of the composite membranes to resist deformation without cracking. If the amount of AgNP added is more than 100 µg, the membrane becomes weaker and brittle (easily torn)

Fig. 2. a) The pores diameter and b) the pores density of Ch membrane and composite membranes (Ch-AgNP10, Ch-AgNP100 and Ch-AgNP1000).

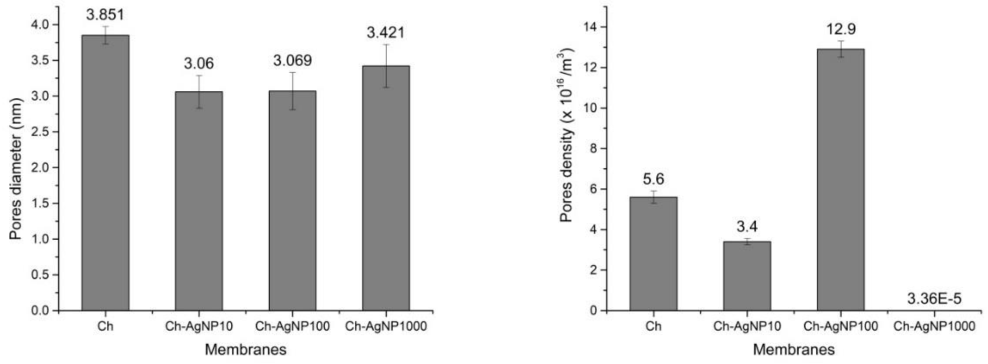

a) b)

Fig. 3. a) Stress-strain curves, b) Elascti modulus (E), c) Tensile strength (TS), and d) elongation at break (ε) of Ch membrane and composite membranes (Ch-AgNP10, Ch-AgNP100 and Ch-AgNP1000) in dry condition.

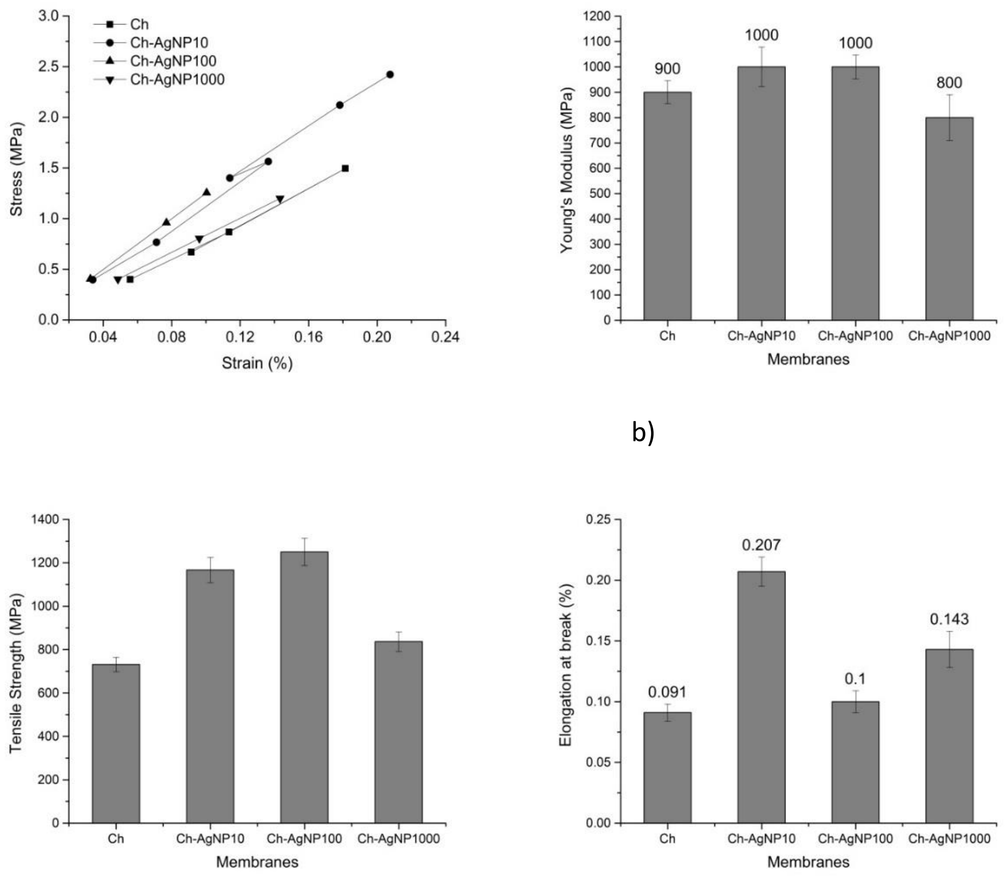

a) b)

c) d)

Water Uptake

Fig. 4a indicates the rate of water of Ch membrane and composite membranes (Ch-AgNP10, Ch-AgNP100, and Ch-AgNP1000). Fig. 4b shows the water uptake maximum of Ch and composite membranes. Fig. 4a shows that in the first 30 minutes, the water uptake of those membranes indicates an increase sharply, the next 30 minutes increased slowly, and then after 60 minutes, the water uptake is reached saturation. Fig. 4a shows that in the first 30 minutes, the water uptake of those membranes indicate a sharp increase, the next 30 minutes increased gently, and then after 60 minutes, the water uptake is reached saturation. Also, it found that the Ch-AgNP100 membrane shows the highest water uptake rate. The maximum water uptake of each membrane is shown in Fig. 4b. It shows that the Ch-AgNP100 showed the highest water uptake. This may be due to the alteration in the hydroxyl group of the composite membrane which was detected in FTIR analysis that shown in Table 1, the OH and amine groups, where water uptake was caused by the formation of hydrogen bonds [8]. This fact is also confirmed by the pores density analysis, where the Ch-AgNP100 has the highest pore density. So, the water uptake ability of the membrane will increase.

Fig. 4. a) The rate of water uptake and b) the water uptake maximum (%) of Ch membrane and composite membranes (Ch-AgNP10, Ch-AgNP100, and Ch-AgNP1000).

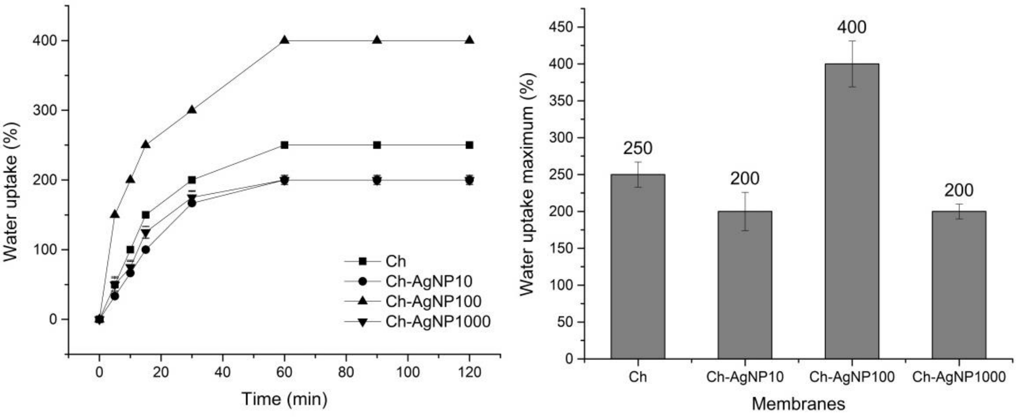

a) b)

Fourier Transform Infrared (FTIR) Analysis

Fig. 5a indicates the FTIR spectra of Ch membrane and composite membranes. For a clearer view, the FTIR spectrum of Ch membrane is redrawn in Fig. 5b. The FTIR spectra found were similar to the spectra reported by other researchers [27], [28]. The analysis is written in Table 1.

Fig. 5. a) The FTIR spectra of Ch membrane and composite membranes (Ch-AgNP10, Ch-AgNP100, and Ch-AgNP 1000), b) The FTIR spectrum of Ch membrane.

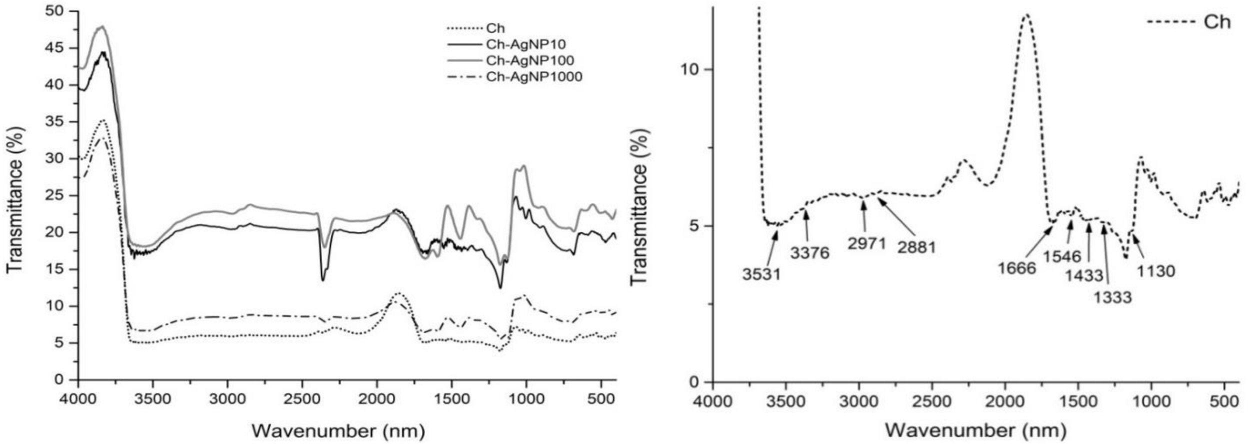

a)

b)

Table 1. The main bands observed in Ch membrane and composite membranes.

Functional Groups*	Wavenumbers presented in Ch and composite membranes, in cm^{-1}; Its transmittance (%)			
	Ch	Ch-AgNP10	Ch-AgNP100	Ch-AgNP1000
–OH stretch	3531; 5.03	3561; 17.40	3538; 18.12	3519; 6.70
–CH_2 stretch	2971; 5.89	2971 (broad); 20.39	2966; 22.53	2953; 8.39
–CH_3 stretch	2881; 6.00	2893; 20.83	2881; 23.24	2888; 8.65
–NH_2 amine group stretch and bend	3376; 5.51 and 1546; 5.31	3317; 20.28 and 1553; 18.04	3305 (shoulder); 21.49 and 1594; 16.72	3310 (shoulder); 8.08 and 1594; 6.74
–C=O stretch of carbonyl group	1666; 5.13	1661; 17.20	1672; 16.44	1672; 6.50
–OH and –CH groups in the pyranose ring	1433; 5.14 and 1333; 5.11	1428; 17.48 and 1333; 17.52	1433;19.16 and 1320; 21.85	1440; 7.15 and 1327; 8.02
The anti-symmetric stretch of C–O–C glycoside link	1130; 4.84	1041; 23.12	1041; 28.41	1046*; 11.02
Metal oxide (Ag-O)	Not observed clearly	582; 19.60	600; 23.00	582; 9.03

*Eun Jung Lee (2004) [34], Monarul (2011) [35].

Fig. 5b shows a broad peak at around 3531 cm^{-1}which is the –OH group stretch. A peak at around 3376 cm^{-1} is the N-H group stretch which is not clearly observed, this may be due to the wide-stretching of -OH so that the N-H group is covered. The presence of the N-H stretching group is in agreement with the presence of bending vibration of the N-H group at a peak around 1546 cm^{-1}. The other peaks include a peak at around 2881 cm^{-1} which is the C-H group stretch, and a peak at around 1666 cm^{-1} is the C=O amide group. These peaks are in agreement with those reported by Eun Jung Lee (2009) [34] and Monarul (2011) [35], the functional groups observed in the chitosan membrane.

The shift of wavenumber and change in the percentage of transmittance in composite membranes spectra were observed from 1666 cm^{-1}. This observation may designate the binding of AgNP to the N-H bond of chitosan [4], [26], [36], [37].

Antibacterial Activity

Fig. 5 and 6 show the antimicrobial activities on S. aureus and E. coli by the forming of a clear zone around samples of Ch membrane and composites membranes. All membranes seem to be highly effective against E. coli growth (clear zone formed) as seen in Fig. 5, but no antibacterial activity was detected on the S. aureus (no clear zone formed), Fig. 6. This antibacterial activity of Ch membrane is in agreement with the work reported in [8] and [4]. These observations indicate the option of considering different antimicrobial mechanisms playing on every type of bacteria [8].

Fig. 5. The inhibitory effect of Ch and composites membranes against gram-negative E.coli, a), b), c), and d).

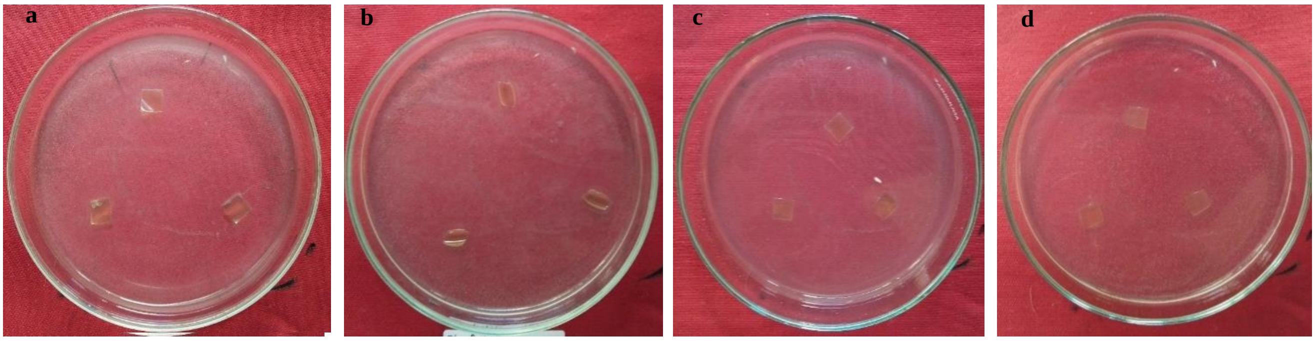

Fig. 6. The inhibitory effect of chitosan and composites membranes against gram-positive bacteria S. aureus, a), b), c), and d).

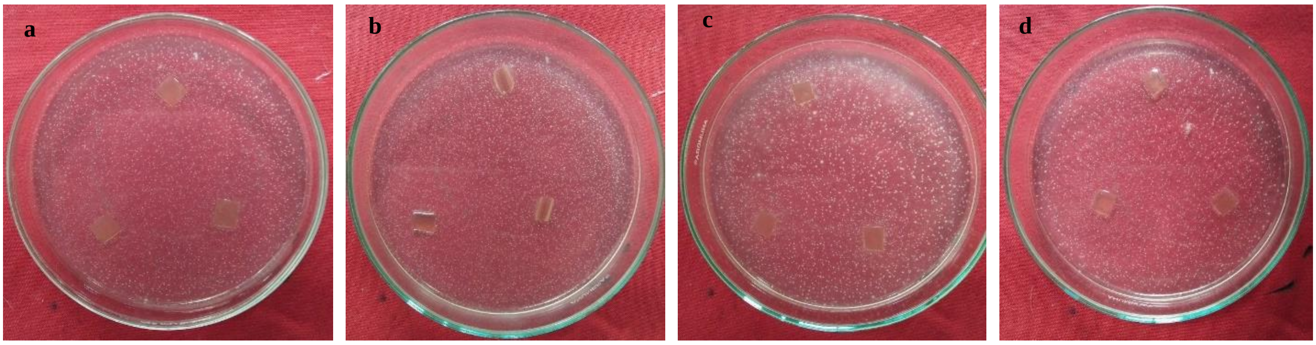

Conclusion

This work has designated the fabrication and characterization of chitosan composite membranes with AgNP as filler to enhance their physical property. The composite membranes were made by casting technique using a solvent of acetic acid 1%. The results showed the diameter of the pores of those composite membranes smaller than the Ch membrane; however, it increased as more amount of AgNP was added. The longest expansion (elongation) is shown by Ch-AgNP100. The highest value of elastic modulus and tensile strength are indicated by membrane Ch-AgNP100 and also it exhibited the highest ability of the water uptake. The XRD pattern of composite membranes showed two peaks 14.89° and 21.27° which relate to the main chitosan, and some new peaks at around 29°, 39°, and 47°, that correspond to AgNP. The functional groups detected in the composite membranes included CH stretch, OH and NH stretch, metal oxide (Ag-O), C=O, and C-O-C which mostly moved to the longer wavenumber compared with Ch membrane. The composite membranes have no antibacterial effect to the S. aureus, but it has effect to E. coli. Referring to these results, it can be deduced that AgNP that added as filler in the manufacturing composite membranes have affected the mechanical properties, crystallinity, and water uptake ability of the composite membranes made. Therefore, this study provided a basic knowledge of the manufacturing of chitosan-AgNP composites membranes with tailored characteristics as well as their application.

REFERENCES

N. N. Rupiasih, M. Sumadiyasa, and I K. Putra, "The Effect of Variations in the Ratio of Matrix/Solvent on the Physical and Mechanical Properties of Chitosan Biopolymer Membranes," IOP Conf. Series: Materials Science and Engineering, vol. 196, 012039, 2017.

N. N. Rupiasih, M. Sumadiyasa, HerySuyanto, and PutriWindari, "Utilization of Shrimp Skin Waste (Sea Lobster) As Raw Material for the Membrane Filtration," IOP Conf. Series: Journal of Physics: Conf. Series, vol. 846, 012003, 2017.

N. N. Rupiasih, YayukEkaPuspita, and M. Sumadiyasa, "Transport phenomena in chitosan synthetic membranes with emphasis on the effect of variations in the ratio of matrix/solvent," Journal of Physics: Conference Series, vol. 622, 012004, 2015.

S. Akmaz, E. D. AdJgüzel, M. Yasar, and O. Erguven, "The Effect of Ag Content of the Chitosan-Silver Nanoparticle Composite Material on the Structure and Antibacterial Activity," Advances in Materials Science and Engineering, pp. 1-6, 2013.

X. Zhang, X. Geng, H. Jiang, J. Li, and J. Huang, "Synthesis and characteristics of chitin and chitosan with the (2-hydroxy-3-trimethylammonium)propyl functionality, and evaluation of their antioxidant activity in vitro," Carbohydrate Polymers, vol. 89, pp. 486-491, 2012.

Ni NyomanRupiasih, Made Sumadiyasa, I Ketut Putra, and Ni Made Rasmini, "Study on Transport Properties of Chitosan Membrane in Different Types of Electrolytes", J. Math. Fund. Sci., vol. 50, no. 2, pp. 182-191, 2018.

P. M. Ajayan, L. S. Schadler, and P. V. Braun, "Nanocomposite science and technology," Weinheim: Wiley-VCH, pp. 239, 2006.

X. Huang, X. Bao, Y. Liu, Z. Wang, and Q. Hu, "Catechol-Functional Chitosan/Silver Nanoparticle Composite as a Highly Effective Antibacterial Agent with Species-Specific Mechanisms," Scientific Reports, vol. 7, pp. 1860, 2017.

M. Thirumavalavan, and J. F. Lee, "A Short Review on Chitosan Membrane for Biomolecules Immobilization," J. Mol. Genet. Med, vol. 9, no. 3, pp. 178, 2015.

M. M. Beppu, C. C. Santana, "In vitro biomineralization of chitosan," Key Eng. Mater., vol. 31, pp. 192-195, 2001.

X. Zeng, and E. Ruckenstein, "Supported chitosan-dye affinity membranes and their protein adsorption," J. Membr. Sci., vol. 117, pp. 271-278, 1996.

Q. L. Hu, Z. P. Fang, Y. Zhao, and C. W. Xu, “A new method to prepare chitosan membrane as a biomedical material,” Chinese J. Poly. Sci., vol. 19, pp. 467-470, 2001.

M. M. Beppu, E. J. Arrud, R. S. Vieira, and N. N. Santos, “Adsorption of Cu(II) on porous chitosan membranes functionalized with histidine,” J. Membr. Sci., vol. 240, pp. 227-235, 2004.

R. Laus, T. G. Costa, B. Szpoganicz, and V. T. Fávere, “Adsorption and desorption of Cu(II), Cd(II) and Pb(II) ions using chitosan crosslinked with epichlorohydrin-triphosphate as the adsorbent,” J. Hazard Mater, vol. 183, pp. 233-241, 2010.

R. Lieder, M. Darai, G. Orlygsson, and O. E. Sigurjonsson, “Solution casting of chitosan membranes for in vitro evaluation of bioactivity,” BiolProced Online, 15, pp. 11, 2013.

[16] H. Susanto, A. M. Samsudin, N. Rokhati, and I. N. Widiasa, “Immobilization of glucose oxidase on chitosan-based porous composite membranes and their potential use in biosensors,” Enzyme MicrobTechnol, 52, pp. 386-392, 2013.

A. R. Boccaccini, M. Erol, W. J. Stark, and J. F. Mano, “Polymer/bioactive glass nanocomposites for biomedical applications: a review,” Compos. Sci. Technol., vol. 70, pp. 1764-1776, 2010.

G. Lu, L. Kong, B. Sheng, G. Wang, Y. Gong, and X. Zhang, “Degradation of covalently crosslinkedcarboxymethyl chitosan and its potential application for peripheral nerve regeneration,” Eur. Polym. J., vol. 43, pp. 3807-3818, 2007.

P. M. Ajayan, L.S. Schadler, and P. V. Braun, “Nanocomposite science and technology,” Weinheim: Wiley-VCH, p. 239, 2006.

K. Hu, M. K. Gupta, D. D. Kulkarni, and V. V. Tsukruk, “Ultra-Robust graphene oxide-silk fibroin nanocomposite membranes,” Adv. Mater., vol. 25, pp. 2301-2307, 2013.

J. D. Oei, W. W. Zhao, L. Chu, M. N. DeSilva, A. Ghimire, H. R. Rawls, and K. Whang, “Antimicrobial acrylic materials with in situ generated silver nanoparticles,” J. Biomed. Mater. Res. Part B, vol. 100B, pp. 409-415, 2012.

I. X. Yin, J. Zhang, I. S. Zhao, M. L. Mei, Q. Li, and C. H. Chu, “The Antibacterial Mechanism of Silver Nanoparticles and Its Application in Dentistry,” International Journal of Nanomedicine, vol. 15, pp. 2555-2562, 2020.

M. Oves, M. Aslam, M. A. Rauf, S. Qayyum, H. A. Qari, M. S. Khan, M. Z. Alam, S. Tabrez, A. Pugazhendhi, and I. M. I. Ismail, “Antimicrobial and anticancer activities of silver nanoparticles synthesized from the root hair extract of Phoenix dactylifera,” Materials Science and Engineering: C, vol. 89, pp. 429-443, 2018.

M. S. Samuel, S. Jose, E. Selvarajan, T. Mathimani, and A. Pugazhendhi, “Biosynthesized silver nanoparticles using Bacillus amyloliquefaciens application for cytotoxicity effect on A549 cell line and photocatalytic degradation of p-nitrophenol,” J. Photochem. Photobiol., vol. 202, 111642, 2020.

S. Akmaz, E. D. AdJgüzel, M. Yasar, and O. Erguven, “The Effect of Ag Content of the Chitosan-Silver Nanoparticle Composite Material on the Structure and Antibacterial Activity,” Advances in Materials Science and Engineering, pp. 1-6, 2013.

S. W. Ali, S. Rajendran, and M. Joshi, “Synthesis and characterization of chitosan and silver loaded chitosan nanoparticles for bioactive polyester,” Carbohydrate Polymers, vol. 83, no. 2, pp. 438-446, 2011.

N. Wendri, N. N. Rupiasih, and M. Sumadiyasa, “Biosynthesis Of Silver Nanoparticles Using Sambiloto Leaf Extract: Optimization Process And Characterization,” JurnalSainsMateri Indonesia, vol. 18, no. 4, pp. 162-167, 2017.

N. N. Rupiasih, M. Sumadiyasa, and P. E. Winasri, “The Study of the Effect of UV-C Radiation on the Current–Voltage Characteristics of Chitosan Membranes,” in Radiation in Medicine and Biology, edited by P. B. Vidyasagar, S. S. Jagtap, O. Yemul, Pan Stanford, pp. 175-185, 2017.

A. L. Barry, M. B. Coyle, C. Thornsberry, E. H. Gerlach, and R. W. Hawkinson, “Methods of measuring zones of inhibition with the Bauer-Kirby disk susceptibility test,” Journal of Clinical Microbiology, vol. 10, no. 6, pp. 885-889, 1979.

R. C. Goy, O. B. G. Assis, “Antimicrobial Analysis Of Films Processed From Chitosan And N,N,N-Trimethyl chitosan,” Brazilian Journal of Chemical Engineering, vol. 31, no. 3, pp. 643-648, 2014.

J. S. Marques, J. A. O. D. Chagas, J. L. C. Fonseca, and M. R. Pereira, “Comparing homogeneous and heterogeneous routes for ionic crosslinking of chitosan membranes,” Reactive and Functional Polymers, vol. 103, pp. 156-161, 2016.

M. Pieróg, M. Gierszewska-Drużyńska, and J. Ostrowska- Czubenko, “Effect Of Ionic Crosslinking Agents on Swelling Behaviour of Chitosan Hydrogel Membranes,” Progress on Chemistry and Application of Chitin and its Derivatives, vol. 14, pp. 75-82, 2009.

IUPAC, Convention for Nomenclature of Porosity (IUPAC Recommendations 2005). Cambridge (UK), 1972.

E. J. Lee, D. S. Shin, H. E. Kim, H. W. Kim, Y. H. Koh, and J. H. Jang, “Membrane of hybrid chitosan–silica xerogel for guided bone regeneration,” Biomaterials, vol. 30, pp. 743-750, 2009.

M. M. Islam, S. M. Masum, M. M. Rahman, M. A. I. Molla, A. A. Shaikh, and S. K. Roy, “Preparation of Chitosan from Shrimp Shell and Investigation of Its Properties,” International Journal of Basic & Applied Sciences, vol. 11, no. 1, pp. 77-80, 2011.

A. Murugadoss, and A. Chattopadhyay, “A “green” chitosan silver nanoparticle composite as a heterogeneous as well as micro-heterogeneous catalyst,” Nanotechnology, vol. 19, no. 1, 2008.

D. Wei, W. Sun, W. Qian, Y. Ye, and X. Ma, “The synthesis of chitosan-based silver nanoparticles and their antibacterial activity,” Carbohydrate Research, vol. 344, pp. 2375-2382, 2009.